Meteorologische Zeitschrift, Vol. 26, No. 2, 147–160 (published online January 24, 2017)

Towards nowcasting of winter precipitation: The Black Ice Event in Berlin 2014

Silke Trömel[1*], Alexander V. Ryzhkov[2], Theresa Bick[3], Kai Mühlbauer[1] and Clemens Simmer[1]

[1]Meteorological Institute of the University of Bonn, Germany
[2]Cooperative Institute for Mesoscale Meteorological Studies, University of Oklahoma, Norman, Oklahoma, and NOAA/OAR/National Severe Storms Laboratory, Norman, Oklahoma
[3]Deutscher Wetterdienst, Offenbach, Germany

(Manuscript received January 15, 2016; in revised form October 4, 2016; accepted October 14, 2016)

Abstract

Prediction of winter precipitation is challenging because besides its amount also its variable phase might have a strong impact on people, transportation, and infrastructure in general. We combine a bulk microphysics numerical weather prediction with a 1D spectral bin microphysical model, which explicitely treats the processes of melting, ice nucleation and refreezing as a first step towards a potential nowcasting application. Polarimetric weather radar observations from the German national meteorological service (DWD) are used to evaluate the approach. The potential of the strategy is demonstrated by its application to the black ice event occurring in Berlin, Germany, on 20 January 2014. The methodology is able to clearly identify the classical mechanism leading to freezing rain at the surface, which might be exploited in future nowcasting algorithms.

Keywords: Winter precipitation, radar polarimetry, nowcasting, spectral bin microphysical model

1 Introduction

The prediction of the location of the rain/snow boundary at the surface, i.e. the transitional area at the surface where pure rain changes to pure snow, and its progression in time are important information for the public, transportation, and the management of infrastructure in general as well as the knowledge on where and when the occurrence of freezing rain at a surface changes to ice pellets or vice versa. The accumulation of rain freezing on contact with the surface over time can cause – beside the obvious effects of slippery roads and runways – extensive damage to trees and power lines, because the weight of the ice may exceed their loading capacity, or to aircrafts by weight increase and changing their wing profiles during landing at or departing from an airport.

Especially the occurrence of freezing rain or ice pellets at the surface depends on minor changes in the vertical thermodynamic profile which the individual hydrometeors experience. Fig. 1 shows median vertical profiles of temperature associated with freezing rain and ice pellets based on a 10-year record of soundings at a number of U.S. locations, where surface temperature was lingering around 0 °C and transitional winter precipitation of various types was observed and well documented (Reeves et al., 2014; Ryzhkov et al., 2014a). Obviously the profiles related to freezing rain and ice pellets are almost indistinguishable near the surface and the maximal temperature difference between them is only about 2 °C in the melting layer.

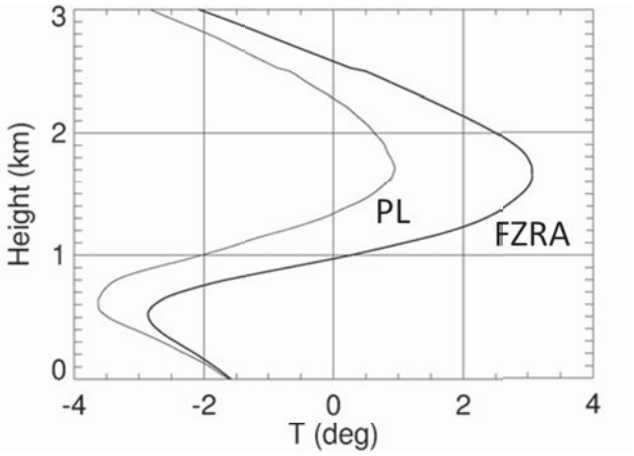

Figure 1: Median low altitude profiles of temperature for freezing rain (FZRA) and ice pellets (PL). This figure is adapted from Fig. 1 in Ryzhkov et al. (2014a).

The accurate modeling of the processes related to the phase of hydrometeors at the surface requires the actual particle size distribution and so-called bin models in order to be able to follow the fate of individual particles from the generation region through the changing environment when they fall towards the ground. Current numerical weather prediction (NWP) models, however, still have to use bulk microphysics schemes for the simulation of microphysical cloud and precipitation processes, which represent the particle size distributions

*Corresponding author: Silke Trömel, Meteorological Institute of the University of Bonn, Auf dem Hügel 20, 53121 Bonn, Germany. Email address: silke.troemel@uni-bonn.de

DOI 10.1127/metz/2016/0778
Gebrüder Borntraeger Science Publishers, Stuttgart, www.borntraeger-cramer.com

usually by only one moment (usually the slope of an exponential function) or two moments at best, partly because of IT constraints.

One major deficiency of bulk microphysics is an inadequate treatment of melting and refreezing of hydrometeors. Even the most sophisticated models use primarily the vertical thermodynamic profiles to identify "warm" atmospheric layers where the melting of snowflakes occurs and "cold" layers where completely or partially melted snowflakes undergo refreezing (Thompson et al., 2004, 2006; Milbrandt and Yau, 2005; Morrison et al., 2015). However, the degree of melting/refreezing crucially depends also on the residence time of the particles in such layers, which may vary dramatically depending on their fall velocity, which in turn is a strong function of particle size, density, shape, and phase composition. Models using bulk microphysics essentially ignore such dependencies.

The most common atmospheric stratification favoring freezing rain and/or ice pellets/sleet is a temperature inversion with above-freezing temperatures above a subfreezing temperature layer beneath which reaches down to the surface. Note, that there are different meanings of the word "sleet" in the U.S.A. and Europe. In the U.S.A., this term refers to ice pellets (Stewart et al., 2015), while in Europe "sleet" describes partially melted and rimed hydrometeors. Since a methodology developed in the U.S.A. is applied in this analysis, their definition is used in the following. Snowflakes may melt completely or partially in the elevated melting layer and potentially refreeze in the subfreezing surface layer. Partially melted snowflakes will start refreezing while encountering the subfreezing layer; completely melted snowflakes (rain or drizzle particles), however, may just become supercooled because ice nucleation requires colder temperatures to activate the ice nuclei inside the drops. In the latter case the supercooled drops will freeze on impact with the surface, power lines, tree branches, or airplanes flying at low altitudes in airport terminal areas causing dangerous icing (e.g., Stewart et al., 2015; Bernstein et al., 2000; Keis, 2015). If raindrops completely refreeze in the subfreezing layer, harmless ice pellets will fall on the ground. Freezing rain can develop either through the described classical cold cloud processes or by supercooled warm-rain processes (Rauber et al., 2000). In the latter situation water vapor may condense into drizzle-size liquid particles at subfreezing air temperatures, which will not freeze at temperatures above $-5 - -6\,^{\circ}\mathrm{C}$ because ice nucleation might be completely missing. Since the classical process involves a warm layer aloft where snowflakes melt and thus produce a melting layer, these situations might be easily detected with polarimetric radars; the latter situation, however, will not show similar distinct signals. The different behavior of completely and partly melted hydrometeors in subfreezing layers is ignored in operational NWP models such as COSMO-DE or RAP and HRRR (Doms and Schättler, 2002; Baldauf et al., 2011; Benjamin et al., 2016).

Due to their area-covering, high-resolution observations weather radars allow for an appropriate sampling of the typically short system lifetimes caused by the often convective nature of precipitation processes also at winter time. Since whole system evolutions are monitored, also nowcasting and short-term predictions up to several hours are possible, which still outperform NWP due to uncertainties in the required initial state (Lin et al., 2005) and time constraints. Moreover, the multidimensional signatures of the polarimetric moments Z_H, Z_{DR}, K_{DP}, and ρ_{HV} (explanations see below) may serve as proxies for many microphysical processes (Trömel and Simmer, 2012) and can help to distinguish between different precipitation types, and to identify transition zones between types and thus also improve quantitative precipitation estimation (Zrnić and Ryzhkov, 1999).

Polarimetric observations are increasingly becoming available operationally; examples are the dual-polarization upgrade of the German national meteorological service (DWD) C-band radar network and the upgrade of the United States National Weather Service (NWS) Weather Surveillance Radar 1988 Doppler (WSR-88D) network. In dry aggregated snow, both the specific differential phase K_{DP} (the range derivative in phase difference between the horizontally, H, and the vertically polarized part, V, of the reflected signal) and the differential reflectivity Z_{DR}(the intensity difference of the reflected H and V polarized signals) are both small and almost independent of radar reflectivity Z_H, while in rain both K_{DP} and Z_{DR} increase with Z_H and the cross-correlation coefficient ρ_{HV} (correlation between H and V polarized reflected signals over a temporal sample) is close to one (Ryzhkov and Zrnić, 1998). Since ice pellets show no correlation between Z_{DR} and Z_H, the existence of such a correlation close to the surface excludes ice pellets. Wet snow, which marks the transition from dry snow to rain, is characterized by high Z_H, Z_{DR} K_{DP}, and low ρ_{HV} (the latter due to an increase in particle diversity and resonance effects) similar to the melting layer or bright band signature aloft in stratiform precipitation, where snowflakes transform into raindrops.

These well-known signals have already been cast into various hydrometeor typing schemes by many national weather services. E.g. DWD develops a 10-type fuzzy-logic hydrometeor typing (Hymec) for its C-band radar network following Park et al. (2009), which is also the basis of the hydrometeor classification algorithm (HCA) applied to S-band WSR-88D radars in the U.S.A. Both algorithms use trapezoidal membership functions, which quantify the probability of hydrometeor types; sounding or NWP information (as in Hymec) of the thermodynamic state of the atmosphere help to improve the typing.

Elmore (2011) and Frech and Steinert (2015) found an insufficient performance of HCA and Hymec, respectively, for winter precipitation because refreezing below the bright band was not considered. According to Kumjian et al. (2013) and Ryzhkov et al. (2014a) ice pellets produced by refreezing in winter storms show

sharp peaks in the Z_{DR} and K_{DP} vertical profiles where ice nucleation with subsequent freezing starts. Preferential freezing of small drops and local ice generation are suggested as plausible mechanisms for this signature, which is suggested to diagnose the transition between freezing rain and ice pellets.

Ryzhkov et al. (2014a) suggested a so-called "background classifier" (SBC) for different surface precipitation types based on available thermodynamic profiles and polarimetric observations. Both are fed into a 1D spectral bin microphysical model, which produces hydrometeor profiles including phase, type and precipitation intensity and allows discriminating between rain (RA), snow (SN), freezing rain (FZRA), and ice pellets/sleet (PL) near the surface. Besides the thermodynamic profile, initial particle size distributions (PSDs) of snowflakes including their degree of riming above the melting layer are required, but can be estimated based on polarimetric radar measurements (see Sec. 2).

According to Reeves et al. (2014) the precipitation type algorithms published by Ramer (1993), Baldwin et al. (1994), Bourgouin (2000), Schuur et al. (2012) and Ryzhkov et al. (2014a) reliably distinguish between snow and rain, but mostly fail regarding the distinction between freezing rain (FZRA) and ice pellets (PL) because of faulty assumptions about features separating wet bulb temperature T_w profiles for FZRA and PL. The scheme by Ryzhkov et al. (2014a), which explicitly treats melting and refreezing, showed the best performance in the intercomparison, and was also able to reproduce a realistic refreezing signature in simulated polarimetric radar data based on the output of the scheme.

Recently, Reeves et al. (2016) developed an augmented version of SBC with snow subdivided into dry and wet snow (SN and RASN) and the mixture of FZRA and PL as a separate class (FZRAPL). The study also addresses the uncertainties related to the variability of the refreezing (ice nucleation) temperature, the degree of riming, the initial size distributions, and the input temperature and humidity profiles.

In this paper we illustrate the potential of the original version of the SBC for classifying winter precipitation during the black ice event in Berlin happening on 20 January 2014 without prior evaluation and adjustment of the scheme for the central European weather regimes. The spectral bin model utilized is simple enough to be operationally implemented, and it has already demonstrated its effectiveness for a large number of storms in comparisons with ground truth as shown in Reeves et al. (2016). The probably most sophisticated cloud model that is focused on transitional winter precipitation was developed by Theriault and Stewart (2010). This is a bulk model built on an existing bulk microphysics scheme of Milbrand and Yau (2005) with additional precipitation categories such as refrozen wet snow, slush, and ice pellets of two different kinds. As a bulk model, however, it does not explicitly treat the variation of the liquid water fraction across the size spectrum and its dependence on the degree of melting/refreezing.

Section 2 shortly introduces the one-dimensional spectral (bin) model for winter precipitation types developed by Ryzhkov et al. (2014a). In Section 3, we describe the synoptic setting of the black ice event in Berlin while Section 4 presents the results of the methodology when applied to the event. Section 5 concludes with a discussion and perspectives for nowcasting.

2 The spectral bin classifier

The one-dimensional spectral (bin) model simulates the profiles of mass contents of water and ice in mixed precipitation for arbitrary vertical thermodynamic profiles and initial distributions of snowflake size and density aloft. Predicted are four near-surface precipitation types: rain (RA), snow (SN), freezing rain (FZRA), and ice pellets (PL). The model explicitly treats melting, ice nucleation and refreezing but assumes no interactions between falling particles such as riming or aggregation, i.e. one ice particle aloft produces a single (potentially mixed-phase) particle at the surface. Thermodynamic profiles can be supplied from NWP or soundings. The initial snowflake size distribution above the melting layer including their degree of riming must be provided, e.g. based on polarimetric radar measurements.

The model starts by assuming a distribution of melted diameters D_W of snowflakes at the surface $N(D_w)$ estimated from the radar reflectivity factor Z_H measured near the surface. In principle, initial PSDs can be estimated from Z_H and Z_{DR}; currently generic raindrop size distributions (DSDs) for different values of Z_H obtained from the analysis of a 7-year disdrometer dataset obtained in central Oklahoma (Schuur et al., 2005) are used. All DSDs were binned into 5 dBZ-wide Z_H classes and for each class a median size distribution was computed and attributed to the respective Z_H observation (Fig. 2). The corresponding size distribution of snowflakes above the melting layer is estimated using particle flux conservation during the snow-to-rain transition in that melting layer (ML) as specified in Zhang et al. (2011) assuming a certain degree of snow riming (Ryzhkov et al., 2014a). The degree of snow riming can potentially be estimated from Z_{DR} just above the ML or from backscatter differential phase δ (to be distinguished from the propagation differential phase change indicated by K_{DP}) and the circular depolarization ratio CDR (the ratio of the powers of the co-polar and cross-polar components of the reflected signal of a circularly emitted wave) within the ML (Ryzhkov et al., 2008; Trömel et al., 2014; Ryzhkov et al., 2014b; Vogel et al., 2015; Kumjian et al., 2016); but due to the still very experimental state of these developments we here simply assume unrimed snow aloft and initial snowflake size distributions corresponding to the average generic rain DSD for Z = 25 dBZ (lowest curve in Fig. 2). This choice

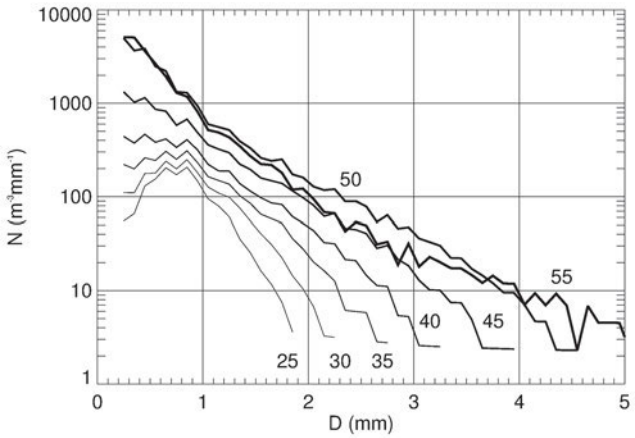

Figure 2: Median DSDs for different radar reflectivity classes (numbers are the related Z_H in dBZ) estimated from a large Oklahoma dataset. This figure corresponds to Fig. 6 in Ryzhkov et al. (2014a).

is well justified for this particular weather event, as will be shown in Section 3 (see Reeves et al. (2016) for a detailed sensitivity study).

The model simulates particle phase transformation and size evolutions for 80 size bins of snowflakes with equivalent melted diameters of $D_w = 0.05 + j\Delta D_w$ ($j = 0, \ldots 79$) with bin sizes of $\Delta D_w = 0.1$ mm. We assume that the initial density of snowflakes ρ_s is a function of their size as specified in Brandes et al. (2007), and that ρ_s can not exceed a threshold of 0.5 g cm^3. In our model experiment, initial dry snowflakes are placed at 3 km height, which is supposed to be at subfreezing temperatures above the ML or above an elevated warm layer. We use a height increment of 10 m, hence we need to determine all relevant variables at 301 height levels down to the surface. For further details of the spectral bin model, we refer to Ryzhkov et al. (2014a) and Reeves et al. (2016).

3 The 2014 black ice event in Berlin

On 20 January 2014, a freezing rain event occurred in Berlin and literally paralyzed the German capital for several hours (daily press, e.g. ZEITonline 2014, Fülling et al., 2014, Jacobs et al., 2014). An extended trough was located over central Europe (Fig. 3). Germany was situated right in the center of the trough in a region with low pressure gradients, where weak southerly flow prevailed. Near the surface, easterly flow dominated the northern part of Germany. This easterly flow resulted from a weak low over the Bavarian forest (center pressure around 1000 hPa) and an intense and cold high pressure zone extending from Finland to Russia. The continental air mass within that anticyclone was dry; the humid air mass located over Germany, however, has been advected from the Mediterraneum at the front side of the cyclone over Bavaria. The concurrence of low altitude cold air from the Scandinavian high-pressure system "Benjamin" coming from the North and higher altitude warmer air from low-pressure systems in the South caused drizzle in the night – and the inversion responsible for contact freezing. Since roads and pavements were at subfreezing temperature the rain immediately froze into a coat of ice and transformed them into a skating rink. The Berlin newspaper (Berliner Zeitung, BZ) reported that 1,182 calls were made to the emergency services by 1 pm. Fire crews were called to 600 incidents between midnight and 10 am. Black ice caused chaos on the roads – between 8 am and 9 am the police was called to 108 traffic accidents in the capital.

DWD distinguishes between simple warnings, warnings due to striking weather and severe weather warnings (DWD, 2015). A warning due to striking weather was passed first at 8:53 am local time (7:53 UTC), i.e., about one hour after the onset of precipitation and a series of accidents. In the following we will elucidate the possible reasons for the rather late warning and demonstrate the potential of dual-polarization radars for icing condition detection if combined with temperature stratification information and the spectral bin model introduced in Section 2.

4 Application the spectral bin model and validation with polarimetric radars

Atmospheric profiles predicted by the NWP model COSMO (Consortium for Small-scale Modeling, for details see Doms and Schättler (2002), or Baldauf et al. (2011) of DWD are used as input for the 1D bin model in order to evaluate whether its application to predicted thermodynamic profiles would have justified an earlier warning. COSMO is a limited-area non-hydrostatic model for NWP, and its configuration COSMO-DE is a particular model setup covering Germany and neighbouring countries with a numerical grid of 2.8 km horizontal resolution and 50 layers, which are terrain-following close to the surface and gradually become horizontal with increasing height. The Lin-type one-moment bulk microphysics scheme simulates five different hydrometeor classes (cloud drops, cloud ice, rain, snow, graupel. Lin et al.,1983; Rheinhardt and Seifert, 2006).

The COSMO-DE simulation was initialized at 06:00 UTC based on the operational analysis and run for 18 hours until 00:00 UTC 21 January 2014. Fig. 4 compares the closest radiosounding from Lindenberg (66 km to the east of Berlin city center) from 6 UTC with the predicted COSMO-DE temperature profile at the location of the Prötzel radar (52.65° N, 13.86° E, Brandenburg, to the north-east of Berlin) also at 06:00 UTC. Observed and modeled profiles compare well and were typical for the classical freezing rain mechanism. Fig. 5 shows the vertical profiles of mass water fraction predicted by the 1D spectral bin model for particles with melted diameters of 1 mm and 3 mm using the observed (thick lines) and the modeled profiles at 06:00 UT (thin

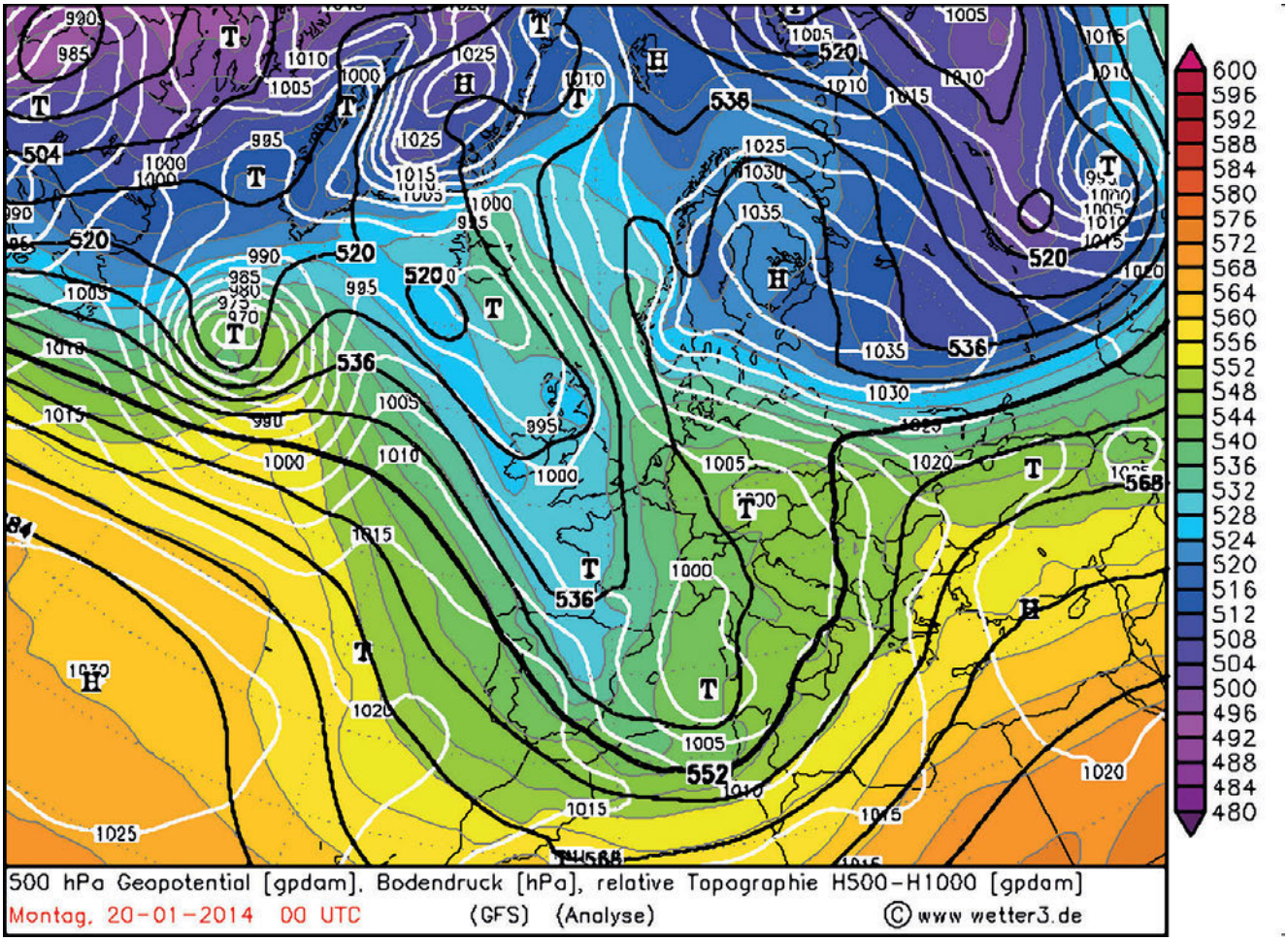

Figure 3: The synoptic weather regime over Europe at 00:00 UTC 20 January 2014 as obtained from the analysis of the Global Forecast System (GFS) model. 500 hPa geopotential height fields (black lines) are overlaid on the surface pressure field (in hPa, white lines), and colors indicate the relative topography 500 hPa–1000 hPa (Source: www.wetter3.de/Archiv).

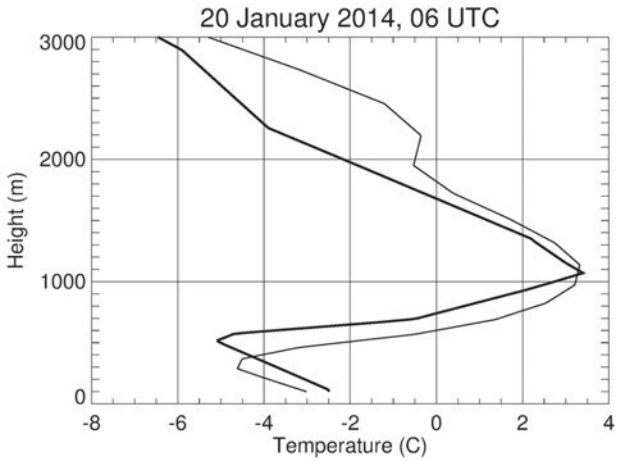

Figure 4: Vertical profiles of temperature retrieved from the COSMO model (thin curve) at the location of the Prötzel radar (52.65 ° N, 13.86 ° E, NE of Berlin) and sounding in Lindenberg (thick curve) at 06:00 UTC 20 January 2014.

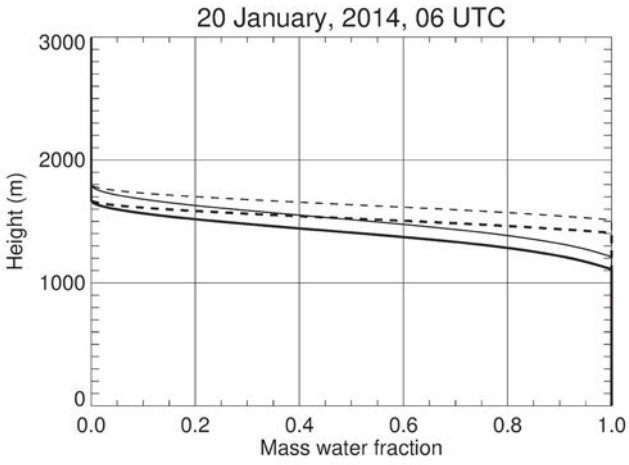

Figure 5: Vertical profiles of mass water content of particles with melted diameter of 1 mm (dashed lines) and 3 mm (solid lines) retrieved from the SBC model using input from the COSMO model (thin curves) and sounding in Lindenberg (thick curves) on 20 January 2014 at 06:00 UTC.

lines), respectively. Accordingly, any snowflake with a melted diameter less than 3 mm would melt completely below the freezing level for both types of profiles. Hence, one can conclude that the warm layer aloft was sufficiently deep to allow complete melting of all snowflakes and the cold surface layer beneath was too warm to activate the ice nuclei in the drops. As a result, both the observed and predicted atmospheric states suggest high surface icing hazard potential.

DWD probably did not issue any warnings, because no precipitation was actually predicted by the model. Inspection of the polarimetric Prötzel radar observations does, however, indicate precipitation. Its plan position indicator (PPI, azimuthal scan) at lowest elevation (0.5°) of Z_H at 06:48 UTC (Fig. 6, upper left panel) clearly shows a precipitation cell approaching the Berlin area with reflectivities above 20 dBZ. Unfortunately, the area of interest is not completely montitored by the Prötzel radar. It was in preoperational mode during that time and azimuths 233°–246° have been omitted to not disturb the still operational Berlin radar. However, the Prötzel radar shows the precipitation cell before and after passing the blind sector and area-wide precipitation sums can be provided by the DWD radar network with 17 overlapping radars (compare Fig. 9). The whole PPI scan at El = 0.5° is below the melting level in a layer of subfreezing temperatures. Raindrops show an increase in oblateness with increasing equivolume diameter. Thus, the increase in Z_H with increasing size of the raindrops and the increase in Z_{DR} with increasing oblateness results in a positive correlation between Z_H and Z_{DR} for raindrops. The positive correlation between Z_H and Z_{DR}, visible in Fig. 6, indicates rain (below freezing temperatures!) as the dominant precipitation type. The areas of highest Z_H are at the same time the areas with the highest Z_{DR} values. Since ice pellets show no correlation between both radar variables, the existence of such a correlation close to the surface excludes ice pellets. The PPI at 8.0° (Fig. 7) clearly identifies the melting layer by the ring-like structure of enhanced Z_{DR}. Again, ice pellets can be excluded because no refreezing signature is evident in the Z_{DR} field, which would in that case show up as a second or "fake bright band" closer to the radar in the PPI of Z_{DR}, but also of K_{DP} and ρ_{HV} (Kumjian et al., 2013;, Ryzhkov et al., 2014a).

Also, the quasi-vertical profiles (QVPs) of the radar variables unambiguously indicate the melting layer in ρ_{hv} and Z_{DR} at about 1.4 km above the ground (Fig. 8) and display the positive correlation between Z_{DR} and Z_H below the melting layer, which is indicative of freezing rain taking the subfreezing temperatures into account. QVPs are obtained by azimuthal averaging of the radar data at higher antenna elevation angles (12° elevation in this case) in order to reduce statistical errors. Trömel et al. (2014) first used QVPs to reliably estimate backscatter differential phase δ. Ryzhkov et al. (2016) further expanded the QVP methodology and demonstrated amongst others its benefits to monitor the height of the melting layer and to detect of microphysical processes (see also Xie et al., 2016). Operational weather radars usually do not perform genuine high-resolution range height indicator scans (RHI, scans at different elevations but constant azimuth) and reconstructed RHIs derived from PPIs at different elevations are often hard to interpret due to their low spatial resolution and noisiness. QVPs are easy to generate operationally and provide much more reliable information about the existence of a melting layer and potential refreezing signatures. QVPs are also potentially instrumental for the detection of supercooled liquid water at high altitudes, which may produce icing hazards for aviation (Ryzhkov et al., 2016; Trömel et al., accepted; Xie et al., 2016). Like the PPIs also the QVPs prove in the Berlin black ice event the positive correlation between Z_{DR} and Z_H below the melting layer, which is indicative of liquid rain (at subfreezing temperatures).

While the COSMO-model did not forecast significant rainfall, the radar-derived precipitation estimates clearly show considerable precipitation (Fig. 9), which – given the polarimetric signatures discussed above – has the potential to produce hazardous freezing rain between 07:00 and 08:00 UTC. The radar-derived precipitation rates are based on the terrain-following precipitaton scans of the German radar network (17 sites) available every five minutes. Measured reflectivities are transferred into precipitation rates using five different z-R relations (where z indicates linear reflectivities at horizontal polarization in mm m^{-3} and R the rain rate in mm h^{-1}) distinguishing between stratiform, convective and hail cases. The radar product shows up to 4 mm of rain over the northeast of Berlin. Between 08:00 and 09:00 UTC also the Berlin area obtained precipitation totals up to 3 mm. Compared to the forecast (Fig. 9), the COSMO-DE analysis (after the assimilation of radar data) shows a tendency towards more area-wide precipitation in the Berlin area (Fig. 10). However, only hourly precipitation sums below 0.5 mm during the time period considered are indicated, which is probably not sufficient for a freezing rain hazard.

The radiosounding from Lindenberg at 06:00 UTC and the COSMO forecasts for the morning precipitation hours show no clear drop below −5 °C in the cold layer near the surface. The algorithm by Reeves et al. (2016) includes the temperature T_{ice} at which ice nucleation of supercooled raindrops occurs as an adaptable parameter. They also show that the best correspondence between the SBC model output and surface observations is achieved if T_{ice} is within the −5 °C – −6 °C interval. Note that this parameter needs in-depth evaluation and adjustment for the central European weather regimes before a potential future implementation.

In the radiosounding at Lindenberg the minimum temperature within the cold layer near the surface (approx. 400 m above MSL) showed −5.1 °C, −5.5 °C, −6.5 °C, and again −6.5 °C at 06:00 UTC, 12:00 UTC, 18:00 UTC 20 January and 00:00 UTC 21 January 2014, respectively. Since the radar data showed a weak refreezing signature around midnight, we speculate that a

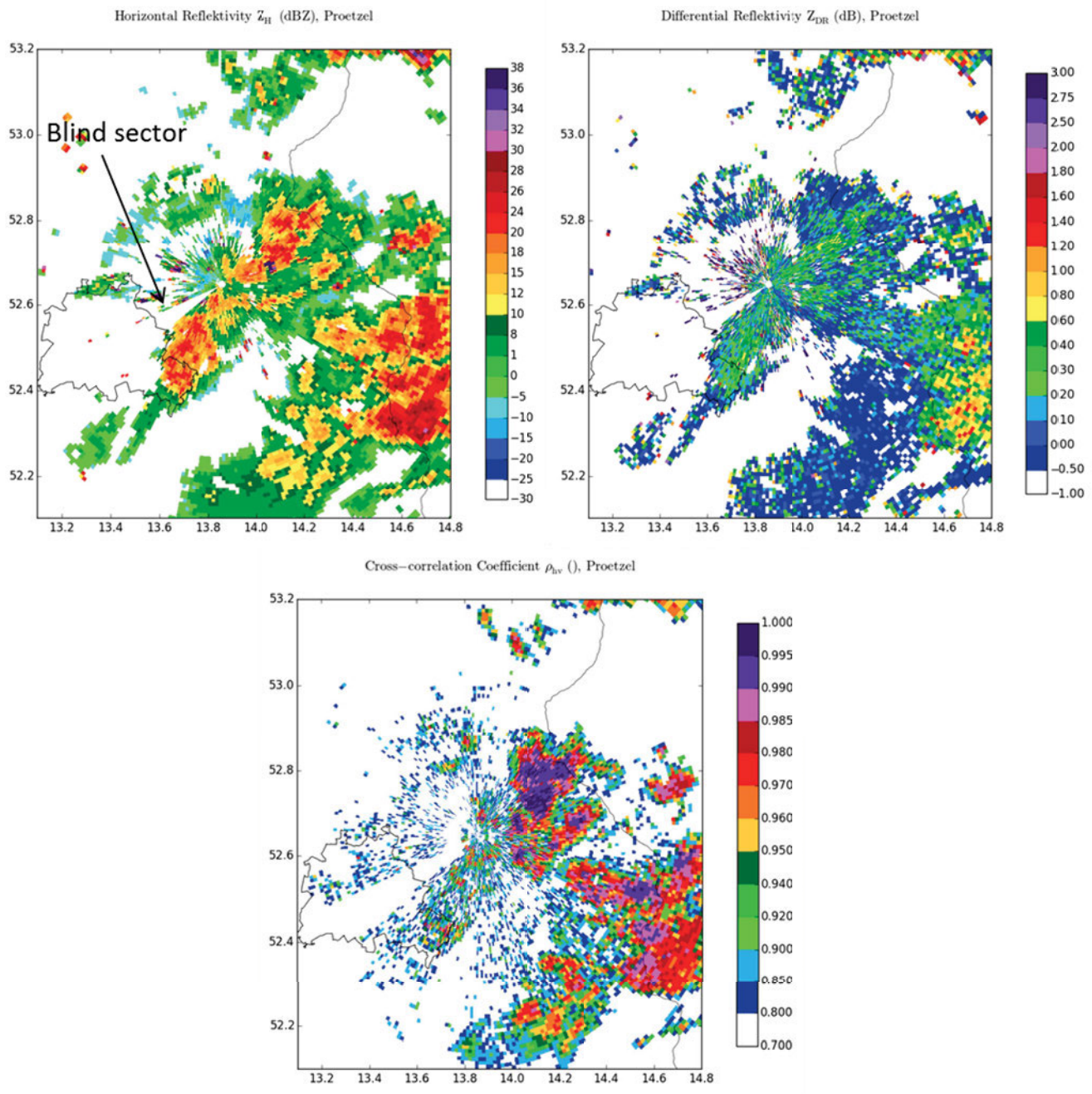

Figure 6: PPIs of Z_H, Z_{DR}, and ρ_{HV} observed at elevation angle 0.5° at 06:48 UTC during the black ice storm with the Prötzel radar (52.65° N, 13.86° E, NE of Berlin) on 20 January 2014.

transition towards ice pellets occurred during the night. However, an earlier transition around 18:00 UTC 20 January is also possible but during that time no significant radar echoes have been observed close to the Prötzel radar at low elevations, which, is mandatory to identify a refreezing signature at heights around 400 m.

Fig. 11 compares the closest radiosounding from Lindenberg at 00:00 UTC 21 January 2014 with the predicted COSMO-DE profile at the location of the Prötzel radar at the same time. Again, observed and modeled profiles compare well with a cold layer at temperatures around T_{ice}. Fig. 12 shows the respective vertical profiles of mass water fraction predicted by the 1D spectral bin model for particles with melted diameters of 1 mm and 3 mm using the observed (thick lines) and the modeled profiles at 00:00 UTC (thin lines), respectively. For snowflakes with melted diameters of 1 mm again the warm layer is sufficiently deep to allow for a complete melting but in contrast to the SBC model output for 06:00 UTC (Fig. 5), the cold surface layer beneath is now cold enough to activate ice nuclei in supercooled drops so that ice pellets may form. Snowflakes with melted diameters of 3 mm, however, would not melt completely in the warm layer and in the cold layer below the SBC model shows a partial (mass water fraction around 0.4) and complete (mass water fraction = 0) re-

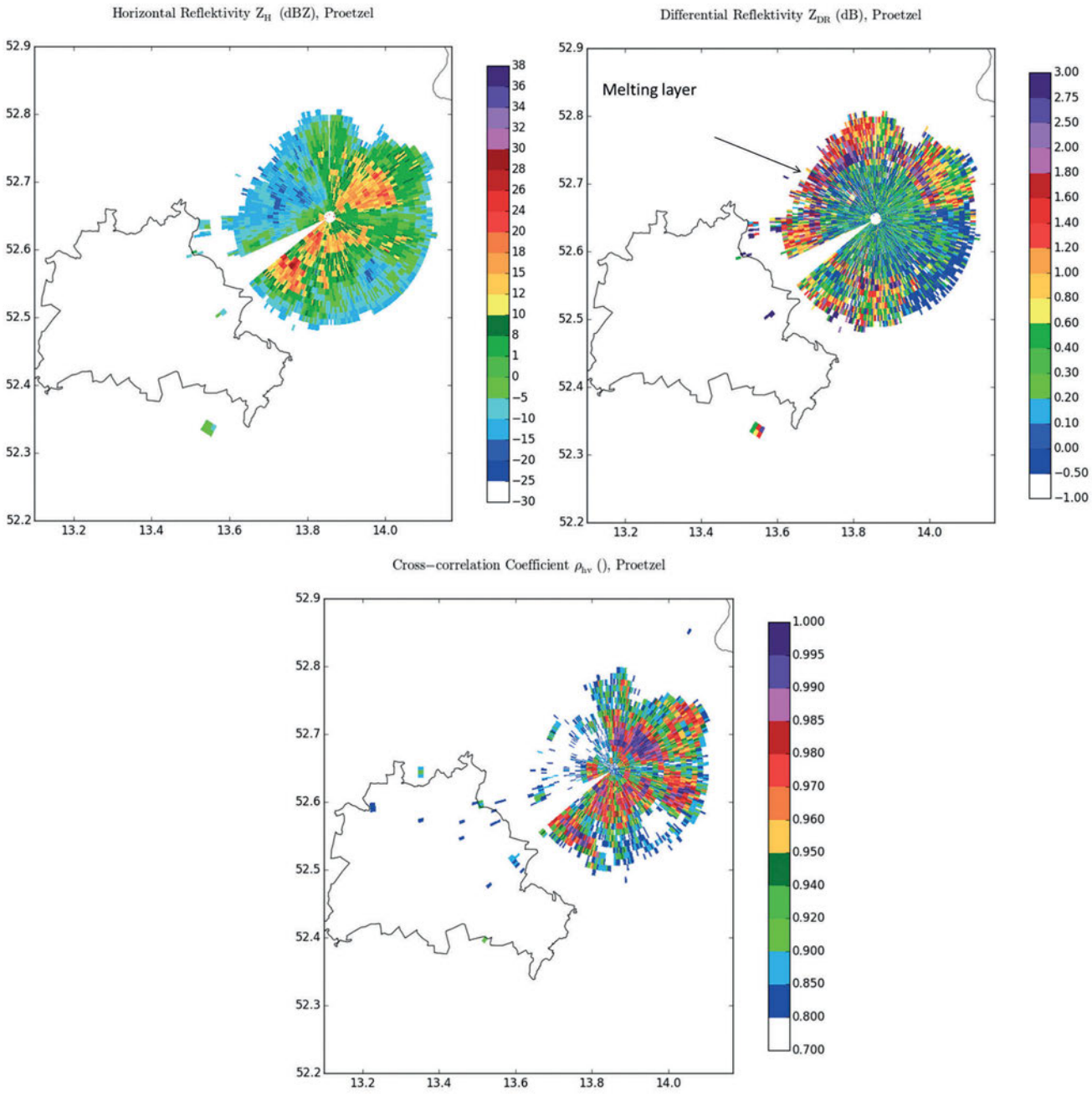

Figure 7: Same as in Fig. 6 but at elevation angle 8.0°.

freezing for the modelled and observed thermodynamic profiles, respectively.

The refreezing process is actually visible, at least for educated eyes, in the PPI of Z_{DR} measured at 3.5° elevation at 23:56 UTC 20 January 2014 (Fig. 13). It is also interesting to note that Z_{DR} reaches magnitudes around 4 dB in the ML indicating high-density, non-aggregated crystals with large aspect ratios (Schuur et al., 2014). In order to make also the refreezing signature more visible, Fig. 14 shows QVPs of Z_H, Z_{DR}, and ρ_{HV}, this time based only on the one PPI shown in Fig. 13 and only on azimuths 1° – 45° with the most pronounced signature included. The refreezing signature is most pronounced in Z_{DR}. The "fake bright band" is detected at around 500 m height, which is consistent with the height of the cold layer in the vertical profile (bottom right panel in Fig. 13 or Fig. 11). Fig. 14 also reveals, despite reduced signal to noise ratio, for refreezing the characteristic decrease in Z_H and ρ_{HV} at around 500 m height. During the freezing rain episode in the morning hours, the emphasized absence of the refreezing signature confirmed that raindrops only have been scanned by the radar, which did not freeze before reaching the surface. In the radar scan measured at 23:56 UTC, however, ice pellets formed above the ground and thus the refreezing signature is visible in the radar measurements. Quite of-

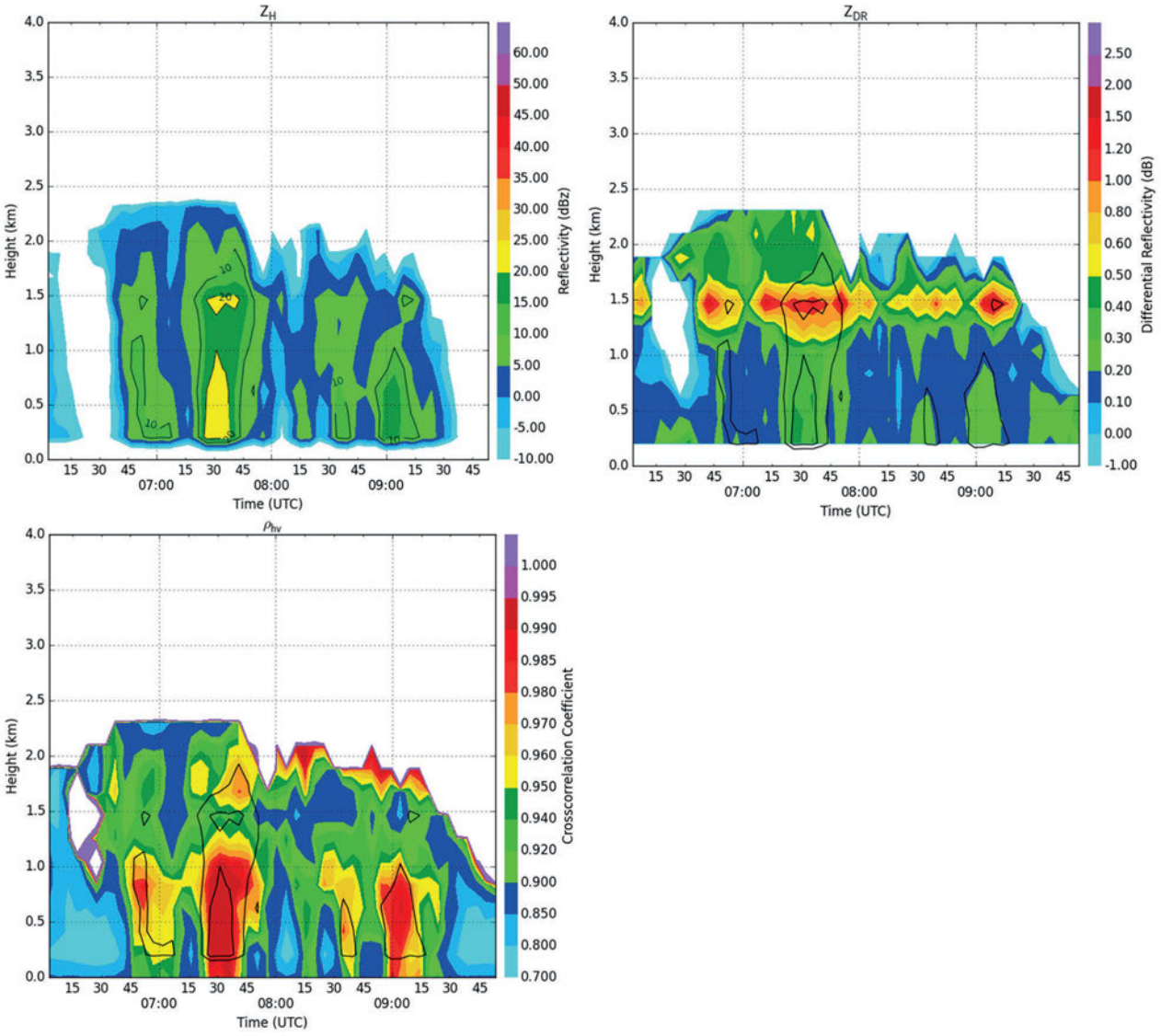

Figure 8: Azimuthal averaged quasi-vertical profiles (QVPs) showing Z_H, Z_{DR}, and ρ_{HV} for the black ice storm between 06:00 and 10:00 UTC. The QVPs are based on the 12° elevation scans of the DWD C band radar in Prötzel, Germany.

ten ice pellets are observed in the transition from freezing rain to snow, like in this case study. Finally, snowfall was monitored the day after the freezing rain hazard, i.e. on 21 January 2014 in Berlin and also the radiosoundings measured in Lindenberg show the thermodynamic profiles typical for snow (compare Reeves et al., 2016) with subfreezing temperatures at all heights.

5 Summary and conclusions

Simulations with a 1D spectral bin microphysical model in thermodynamic environments taken from both observed and modeled thermodynamic profiles during the Berlin black ice event in 2014 clearly indicate a high potential for freezing rain during the morning hours. The available polarimetric radar observations showed precipitation, which was, however, not predicted by the NWP model. The radar observations also did not indicate any signs of refreezing rain in the subfreezing near-surface air below the melting layer. Thus the synergetic use of predicted and/or observed thermodynamic profiles to initiate a spectral bin model results together with polarimetric radar observations could have been exploited in a potential warning scheme.

Of course not always situations will be that unambiguous, thus we suggest – besides testing the described approach for a range of conditions – to make the described method more robust by feeding ensembles of initial snow DSDs including potential riming effects estimated from polarimetric observations above the melting layer to the 1D spectral bin model to achieve a probabilistic pathway to severe winter precipitation hazards. The full implementation of the 1D model, which explicitly treats melting, ice nucleation and refreezing, would then provide probabilities for at least the four near sur-

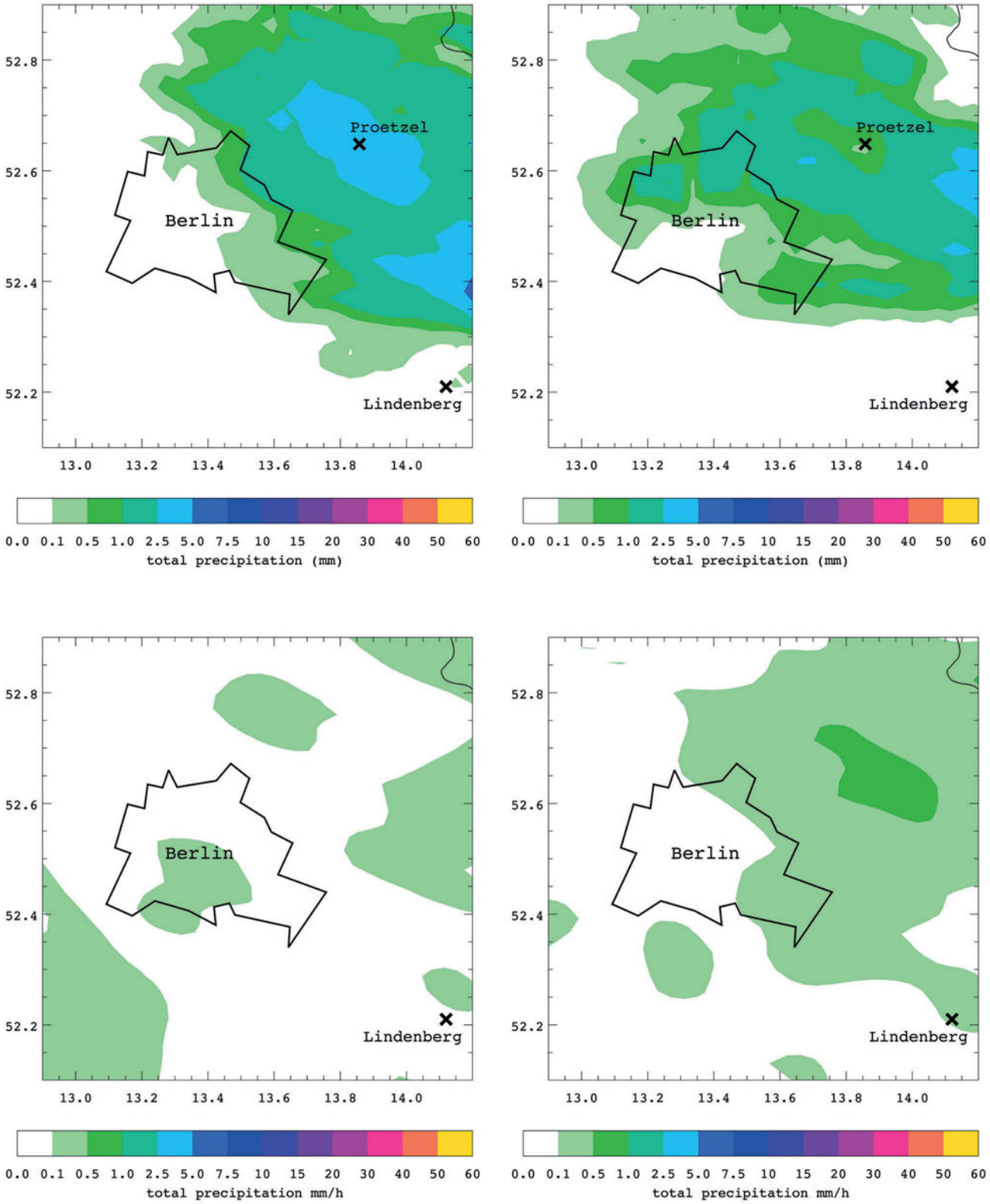

Figure 9: Accumulated surface precipitation sum based on radar observations (top row) and COSMO model output initialized at 6 UTC (bottom row) between 07:00 and 08:00 UTC (left column) and between 08:00 and 09:00 UTC (right column) for the Berlin area on 20 January 2014.

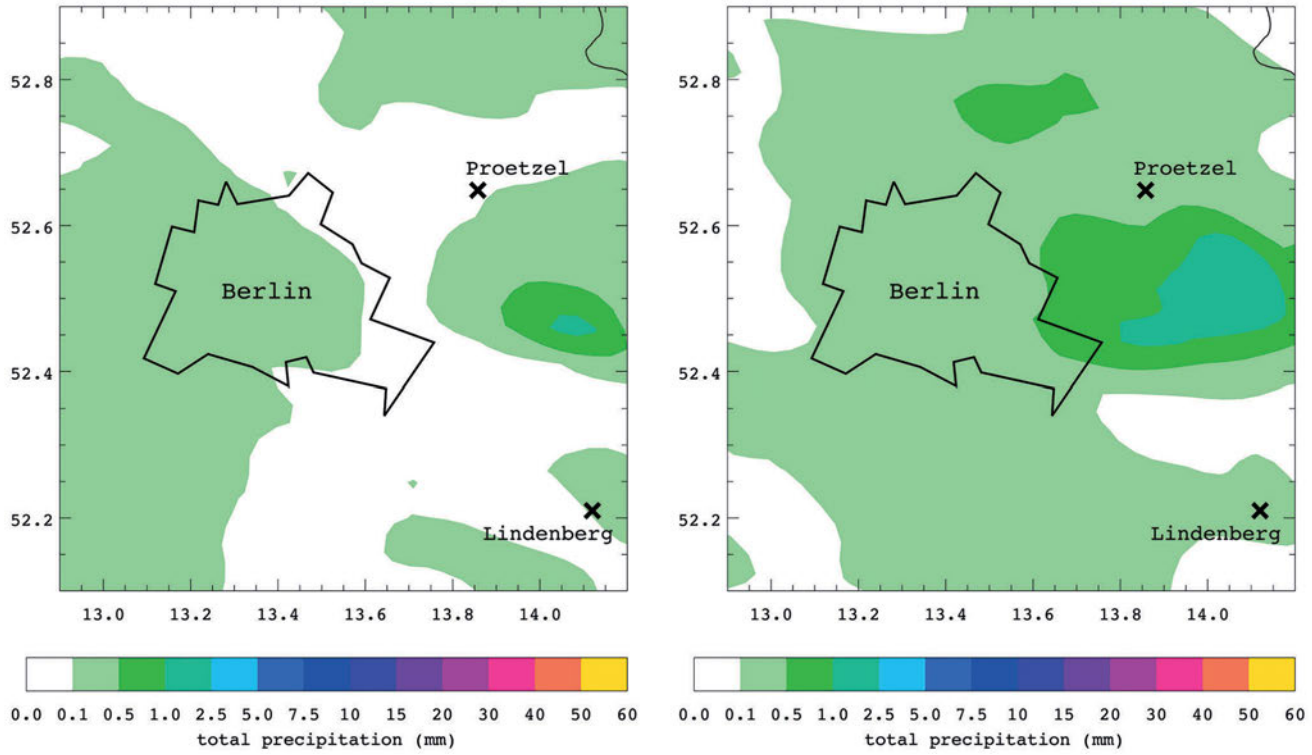

Figure 10: Accumulated surface precipitation sum based on COSMO analysis output (including radar data assimilation) between 07:00 and 08:00 UTC (left) and between 8 and 9 UTC (right) for the Berlin area on 20 January 2014.

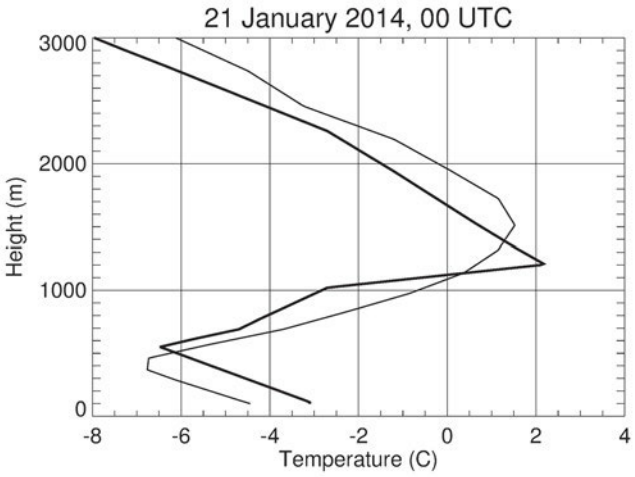

Figure 11: Same as in Fig. 4 but for 00:00 UTC 21 January 2014. Vertical profiles of temperature retrieved from the COSMO model (thin curve) at the location of the Prötzel radar (52.65° N, 13.86° E, NE of Berlin) and the sounding in Lindenberg (thick curve) for the same time.

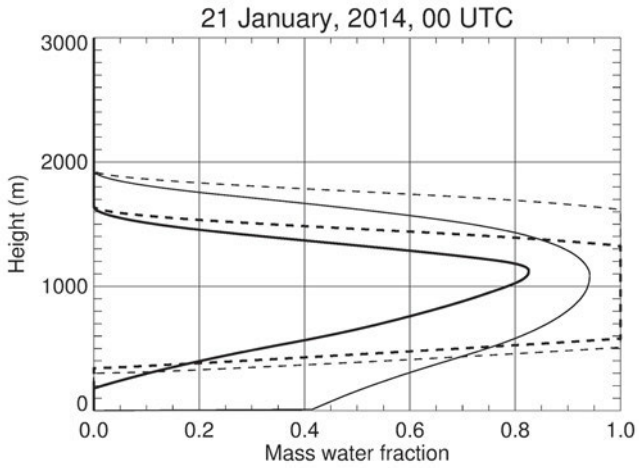

Figure 12: Same as in Fig. 5 but for 00:00 UTC 21 January 2014. Vertical profiles of mass water content of particles with melted diameter of 1 mm (dashed lines) and 3 mm (solid lines) retrieved from the SBC model using input from the COSMO model (thin curves) and sounding in Lindenberg (thick curves) at 00:00 UTC 21 January 2014.

face precipitation types: rain, snow, freezing rain, and ice pellets. A probabilistic approach is required, because the difference between the vertical profiles, which lead to either freezing rain or ice pellets, can be very small as detailed in the introduction and demonstrated with the analysis at around 00:00 UTC 21 January 2014. But the careful exploitation of polarimetric fingerprints could add confidence to any decision.

The described methodology, which we applied to the Berlin black ice event, has been validated already in the U.S.A. with surface observations using Automated Surface Observing Stations (ASOS) by Reeves et al. (2014, 2016) and crowd-sourcing weather reports from the general public via the mPING app for smart phones by Elmore (2014) and Reeves et al. (2016). Reeves et al. (2016), however, does not connect the SBC with polari-

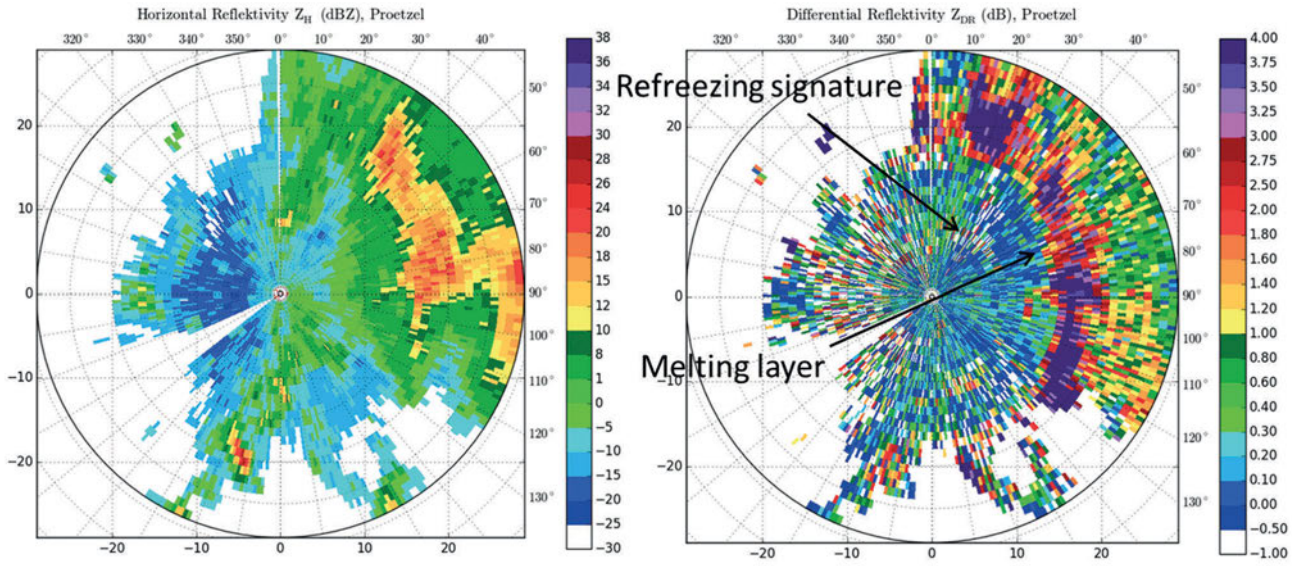

Figure 13: PPIs of Z_H (left), and Z_{DR} (right) at elevation angle 3.5° at 23:56 UTC 20 January 2014 measured with the Prötzel radar (52.65° N, 13.86° E, NE of Berlin). The black arrows point to the melting layer and the refreezing signature, respectively.

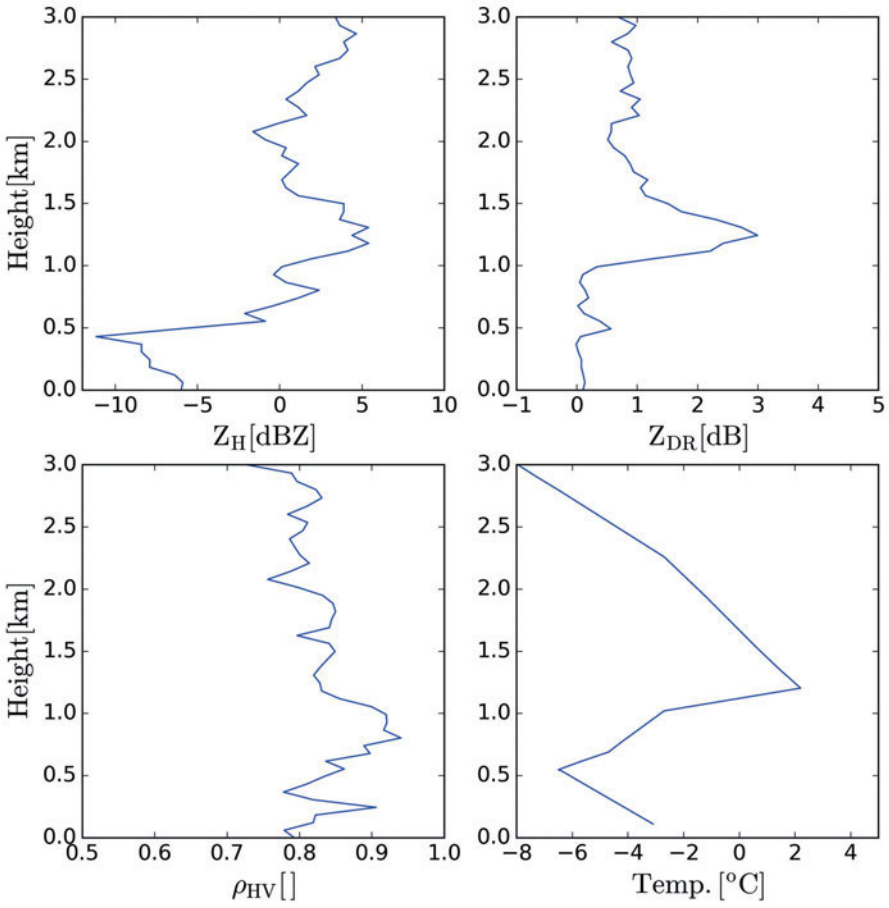

Figure 14: Quasi-vertical profiles (QVPs) of Z_H and Z_{DR} (top row) derived from the 3.5° elevation scan measured at 23:56 UTC 20 January 2014 with the Prötzel radar (displayed in Fig. 13, left panel) via azimuthally averaging of azimuths 1°–45° and transforming the range coordinate into height. Additionally, the QVP of ρ_{HV}, derived from the same scan, and the vertical temperature profile from the sounding in Lindenberg for 00.00 UTC 21 January 2014 are shown (bottom row). The temperature profile already shown in Fig. 11 is reproduced for a direct comparison with the polarimetric variables.

metric radar observations. The case study presented is the first demonstrating the consistency of the SBC output with radar observations and the idea of exploiting the relationship between Z_H and Z_{DR} as well as the refreezing signature for diagnostics and nowcasting. The analysis can be considered as an independent validation of the SBC performance in the European climate regime. Especially the confirmation of the refreezing temperature threshold of −6 °C, which was a debatable issue among cloud physicists for long time, is of great value.

Events like the described one are – fortunately – rare, and thus pose a challenging validation problem for our nowcasting approach. It needs to be shown, whether available disdrometer measurements from the DWD network will satisfy these requirements. The development of a crowd-sourcing app similar to mPing to enhance surface observations for all kinds of severe weather is already underway in Europe, which will strengthen the European Severe Weather Data Base (ESWD, http://www.eswd.eu/) and would provide a valuable data source for the method.

Acknowledgments.

The research of Silke Trömel was partly carried out in the framework of the Hans-Ertel-Centre for Weather Research (http://www.herz-tb1.uni-bonn.de/). This research network of universities, research institutes and the Deutscher Wetterdienst (DWD) (Simmer et al., 2016) is funded by the BMVBS (Federal Ministry of Transport, Building and Urban Development). Alexander Ryzhkov was supported via funding from NOAA/University of Oklahoma Cooperative Agreement #NA11OAR4320072 under the U.S. Department of Commerce and from the National Science Foundation (grant AGS-1143948) and in part by the Transregional Collaborative Research Center TR32 (Simmer et al., 2015). We gratefully acknowledge the support by DWD for providing the polarimetric C-band radar data for Prötzel, Germany, and the national radar-based precipitation product.

References

Baldauf, M., A. Seifert A., J. Förstner, D. Majewski, M. Raschendorfer, T. Reinhardt, 2011: Operational Convective-Scale NumericalWeather Prediction with the COSMO Model: Description and Sensitivities. – Mon. Wea. Rev. **139**, 3887–3905, DOI:10.1175/MWR-D-10-05013.1.

Baldwin, M., R. Treadon, S. Contorno, 1994: Precipitation types prediction using a decision tree approach with NMCs mesoscale eta model. – Preprints. 10th Conf. on Numerical Weather Prediction, Portland, OR, Amer. Meteor. Soc., 30–31.

Benjamin, S., J. Brown, T. Smirnova, 2016: Explicit precipitation-type diagnosis from a model using a mixed-phase bulk cloud-precipitation microphysics parameterization. – Wea. Forecast. **31**, 609–619.

Bernstein, B., 2000: Regional and local influences on freezing drizzle, freezing rain, and ice pellets events. – Wea. Forecast. **15**, 485–508.

Bourgouin, P., 2000: A method to determine precipitation type. – Wea. Forecast. **15**, 583–592.

Brandes, E.A., K. Ikeda, G. Zhang, M. Schoenhuber, R. Rasmussen, 2007: A statistical and physical description of hydrometeor distributions in Colorado snowstorms using a video-disdrometer. – J. Appl. Meteor. **46**, 634–650, DOI: 10.1175/JAM2489.1.

Doms, G., U. Schättler, 2002: A description of the nonhydrostatic regional model LM, Part I: Dynamics and Numerics. – COSMO Newsl. **2**, 225–235.

DWD, 2015: Wetterwarnung. – http://www.dwd.de/bvbw/appmanager/bvbw/dwdwwwDesktop?_nfpb=true&_pageLabel=dwdwww_result_page&gsbSearchDocId=663962.

Elmore, K.L.J., 2011: The NSSL Hydrometeor Classification Algorithm in Winter Surface Precipitation: Evaluation and Future Development. – Wea. Forecast. **26**, 756–765.

Elmore, K., H. Moser, V. Lakshmanan, B. Kaney, H. Reeves, V. Farmer, L. Rothfusz, 2014: mPING: Crowd-sourcing weather reports for research. – Bull. Amer. Meteor. Soc. **95**, 1335–1342.

Frech, M., J. Steinert, 2015: Polarimetric radar observations during an orographic rain event. – Hydrol. Earth Sys. Sci. **19**, 1141–1152.

Fülling, T., A. Gandzior, I. Jürgens, H. Labenski, 2014: Kalt erwischt – Blitzeis überfordert Berliner Rettungskräfte. – http://www.morgenpost.de/berlin-aktuell/article124055778/Kalt-erwischt-Blitzeis-ueberfordert-Berliner-Rettungskraefte.html (last visited 15 September 2015).

Jacobs, S., H. Onken, J. Hasselmann, 2014: Doppelt so viele Einsätze wie normal. – http://www.tagesspiegel.de/berlin/ausnahmezustand-in-berlin-doppelt-so-viele-rettungseinsaetze-als-normal/9354362.html (last visited 15 September 2015).

Keis, F., 2015: WHITE – Winter hazards in terminal environment: An automated nowcasting system for Munich Airport. – Meteorol. Z. **24**, 61–82.

Kopietz, A. 2014: Feuerwehr kritisiert Deutschen Wetterdienst. – http://www.berliner-zeitung.de/berlin/blitzeis-in-berlin-feuerwehr-kritisiert-deutschen-wetterdienst-1544630 (accessed on December 14, 2016).

Kumjian, M., A. Ryzhkov, H. Reeves, T. Schuur, 2013: Dual-polarization radar observations of hydrometeor refreezing in winter storms. – J. Appl. Meteor. Climate **52**, 2549–2566.

Kumjian, M., S. Mishra, S. Giangrande, T. Toto, A. Ryzhkov, A. Bansemer, 2016: Polarimetric radar and aircraft observations of saggy bright band during MC3E. – J. Geophys. Res. Atmos. **121**, 3584–3607.

Lin, Y.L., R.D. Farley, H.D. Orville, 1983: Bulk Parameterization of the Snow Field in a Cloud Model. – J. Climate Appl. Meteor. **22**, 1065-1092, DOI:10.1175/1520-0450(1983)022<1065:BPOTSF>2.0.CO;2.

Lin, C., S. Vasic, A. Kilambi, B. Turner, I. Zawadzki, 2005: Precipitation forecast skill of numerical weather prediction models and radar nowcasts. – Geophys. Res. Lett. **32**, L14801, DOI:10.1029/2005GL023. 451.

Milbrandt, J.A., M.K. Yau, 2005: A multimoment bulk microphysics parameterization. Part II: A proposed three-moment closure and scheme description. – J. Atmos. Sci. **62**, 3065–3081.

Morrison, H., J.A. Milbrandt, G.H. Bryan, K. Ikeda, S.A. Tessendorf, G. Thompson, 2015: Parameterization of Cloud Microphysics Based on the Prediction of Bulk Ice Particle Properties. Part II: Case Study Comparisons with Observations and Other Schemes. – J. Atmos. Sci. **72**, 312–339. DOI: 10.1175/JAS-D-14-0066.1.

Park, H., A. Ryzhkov, D.S. Zrnić, K.E. Kim, 2009: The hydrometeor classification algorithm for the polarimetric WSR-88D: Description and application to an MCS. – Wea. Forecast. **24**, 730–748.

Ramer, J., 1993: An empirical technique for diagnosing precipitation type from model output. – Fifth Int. Conf. on Aviation Weather Systems, Vienna, VA., Amer. Meteor. Soc. 227–230.

Rauber, R., L. Olthoff, M. Ramamurthy, 2000: The relative importance of warm rain and melting processes in freezing precipitation events. – J. Appl. Meteor. **39**, 1185–1195.

Reeves, H., T. Schuur, A. Ryzhkov, K. Elmore, J. Krause, K. Ortega, 2013: Testing of a background classification algorithm for use with dual-polarized radars in determining precipitation type at the surface. – 36th Conference on Radar Meteorology, Breckenridge, CO.

Reeves, H.D., K.L. Elmore, A. Ryzhkov, T. Schuur, J. Krause, 2014: Source of uncertainty in precipitation-type forecasting. – Wea. Forecast. **29**, 936–953.

Reeves, H.D., A. Ryzhkov, J. Krause, 2016: Discrimination between winter precipitation types based on spectral-bin microphysical modeling. – J. Appl. Meteor. Climatol. **55**, 1747–1761. DOI:10.1175/JAMC-D-16-0044.1.

Rheinhardt, T., A. Seifert, 2006: A three-category ice scheme for LMK. – COSMO Newsletter **6**, 115–120.

Ryzhkov, A., D. Zrnić, 1998: Discrimination between rain and snow with a polarimetric radar. – J. Appl. Meteor. **37**, 1228–1240.

Ryzhkov, A., S. Giangrande, A. Khain, M. Pinsky, A. Pokrovsky, 2008: Exploring model-based polarimetric retrieval of vertical profiles of precipitation. – Extended Abstracts, 5th European Conference on Radar in Meteorology and Hydrology, Helsinki, Finland, CD-ROM, P6.1.

Ryzhkov, A., H. Reeves, J. Krause, H. Burcham, 2014a: Discrimination between winter precipitation types based on explicit microphysical modeling of melting and refreezing in the polarimetric hydrometeor classification algorithm. Extended abstract. – The 8th European Conference on Radar in Meteorology and Hydrology, 198, Garmisch-Partenkirchen, Germany, 7 pp.

Ryzhkov, A., P. Zhang, Q. Cao, S. Matrosov, V. Melnikov, and M. Knight, 2014b: Measurements of Circular Depolarization Ratio with the Radar with Simultaneous Transmission/Reception. – The 8th European Conference on Radar in Meteorology and Hydrology, 11.3, Garmisch-Partenkirchen, Germany, 10 pp.

Ryzhkov, A., P. Zhang, H. Reeves, M. Kumjian, T. Tschallener, S. Trömel, C. Simmer, 2016: Quasi-vertical profiles – a new way to look at polarimetric radar data. – J. Atmos. Oceanic Technol. **33**, 551–562.

Schuur, T.J., A.V. Ryzhkov, D.R. Clabo, 2005: Climatological analysis of DSDs in Oklahoma as revealed by 2D-video disdrometer and polarimetric WSR-88D. Preprints, 32nd Conf. on Radar Meteorology, Albuquerque, NM, Amer. Meteor. Soc., 15R.4. [Available online at https://ams.confex.com/ams/pdfpapers/95995.pdf.]

Schuur, T., H. Park, A. Ryzhkov, H. Reeves, 2012: Classification of precipitation types during transitional winter weather using the RUC model and polarimetric radar retrievals. – J. Appl. Meteor. Climate **51**, 763–779.

Schuur, T., A. Ryzhkov, D. Forsyth, P. Zhang, H. Reeves, 2014: Precipitation Observations with NSSL's X-band Polarimetric Radar during the SNOW-V10 Campaign. – Pure Appl. Geophys. **171**, 95–112. DOI:10.1007/s00024-012-0569-2.

Simmer, C., I. Thiele-Eich, M. Masbou, W. Amelung, S. Crewell, B. Diekkrueger, F. Ewert, H.-J. Hendricks Franssen, A.J. Huisman, A. Kemna, N. Klitzsch; S. Kollet, M. Langensiepen, U. Loehnert, M. Rahman, U. Rascher, K. Schneider, J. Schween, Y. Shao, P. Shrestha, M. Stiebler, M. Sulis, J. Vanderborght, H. Vereecken, J. van der Kruk, T. Zerenner, G. Waldhoff, 2015: Monitoring and Modeling the Terrestrial System from Pores to Catchments – the Transregional Collaborative Research Center on Patterns in the Soil-Vegetation-Atmosphere System. – Bull. Amer. Meteor. Soc., published online. DOI:10.1175/BAMS-D-13-00134.1.

Simmer, C., G. Adrian, S. Jones, V. Wirth, M. Göber, C. Hohenegger, T. Janjic, J. Keller, C. Ohlwein, A. Seifert, S. Trömel, T. Ulbrich, K. Wapler, M. Weissmann, J. Keller, M. Masbou, S. Meilinger, N. Riss, A. Schomburg, C. Stein, A. Vormann, 2016: HErZ – The German Hans-Ertel Centre for Weather Research. – Bull. Amer. Meteor. Soc. **97**, 1057–1068. DOI:10.1175/BAMS-D-13-00227.1.

Stewart, R., J. Theriault, W. Henson, 2015: On the characteristics of and processes producing winter precipitation types near 0 °C. – Bull. Amer. Meteor. Soc. **96**, 623–639.

Sun, J., M. Xue, J.W. Wilson, I. Zawadzki, S.P. Ballard, J. Onvlee-Hooimeyer, P. Joe, D.M. Barker, P.-W. Li, B. Golding, M. Xu, J. Pinto, 2014: Use of NWP for Nowcasting Convective Precipitation. – Bull. Amer. Meteor. Soc. **95**, 409–426, DOI:10.1175/BAMS-D-11-00263.1.

Theriault, J., R. Stewart, 2010: A parameterization of the microphysical processes forming many types of winter precipitation. – J. Atmos. Sci. **67**, 1492–1508.

Thompson, G., R.M. Rasmussen, K. Manning, 2004: Explicit Forecasts of Winter Precipitation Using an Improved Bulk Microphysics Scheme. Part 1: Description and Sensitivity Analysis. – Mon. Wea. Rev. **132**, 519–542.

Thompson, G., P.R. Field, W.D. Hall, R. Rasmussen, 2006: A new bulk microphysical parameterization for WRF (& M5). – Paper presented at WRF Conference, Natl. Cent. for Atmos. Res. Boulder, Colo., June.

Trömel, S., C. Simmer, 2012: An object-based approach for areal rainfall estimation and validation of atmospheric models. Meteorol. – Atmos. Phys. **115**, 139–151. DOI: 10.1007/s00703-011-0173-5.

Trömel, S., A. Ryzhkov, P. Zhang, C. Simmer, 2014: Investigations of backscatter differential phase in the melting layer. – J. Appl. Meteor. Climate **53**, 2344–2359. DOI:10.1175/JAMC-D-14-0050.1.

Trömel, S., A. Ryzhkov, M. Diederich, K. Mühlbauer, C. Simmer, S. Kneifel, J. Snyder, accepted: Multi-sensor characterization of mammatus. – Mon. Wea. Rev.

Vogel, J., F. Fabry, I. Zawadzki, 2015: Attempts to observe poalrimetric signatures of riming in stratiform precipitation. – 37th Conf. On Radar Meteorology, Norman, OK, Amer. Meteor. Soc., extended abstracts, 6B.6.

Xie, X., R. Evaristo, C. Simmer, J. Handwerker, S. Trömel, 2016: Precipitation and Microphysical Processes Observed by Three Polarimetric X-Band Radars during HOPE. – Atmos. Chem. Phys. **16**, 7105–7116.

ZEITonline, 2014: Blitzeis sorgt für Ausnahmezustand in Berlin. – http://www.zeit.de/gesellschaft/2014-01/blitzeis-wetter-berlin-brandenburg (last visited 15 September 2015).

Zhang, G., S. Luchs, A. Ryzhkov, M. Xue, L. Ryzhkova, Q. Cao, 2011: Winter precipitation microphysics characterized by polarimetric radar and video disdrometer observations in central Oklahoma. – J. Appl. Meteor. Climate **50**, 1558–1570.

Zrnić, D.S., A.V. Ryzhkov, 1999: Polarimetry for Weather Surveillance Radars. – BAMS **80**, 389–406.